Hollow Out-of-Plane Polymer Microneedles Made by Solvent Casting for Transdermal Drug Delivery

Iman Mansoor, Urs O. Häfeli, and Boris Stoeber, *Member, IEEE*

***Abstract*—Although hollow microneedles have been proposed as an effective and convenient method for transdermal drug delivery, their expensive fabrication techniques to date have prevented their mass fabrication as a viable option. A novel method, based on solvent casting, is presented for inexpensive fabrication of hollow out-of-plane polymer microneedles. Microneedles are formed during a solvent evaporation process, which leaves a polymer layer around pillars in a prefabricated mold. The mold is fabricated using photolithography and can be used for consecutive solvent casting of microneedles. Arrays of microneedles with lengths up to 250 μm have been fabricated from clay-reinforced polyimide. Several mechanical tests were performed on solvent cast solid structures to find the optimum clay percentage in the polyimide that would lead to the highest compressive strength. The fabricated needles were tested for robustness, and it was observed that the needles were capable of withstanding on average compressive loads of up to 0.32 N. The suitability of the microneedles for skin penetration and drug delivery was demonstrated by injection of fluorescent beads into a skin sample. [2011-0200]**

***Index Terms*—BioMEMS, drug delivery, hollow out-of-plane polymer microneedles, solvent-cast microstructures.**

I. Introduction

TRANSDERMAL drug delivery is becoming increasingly popular because it is not associated with the potential risks and pain of traditional hypodermic needles. One method for transdermal drug delivery uses adhesive skin patches. In this method, a pharmaceutical compound is absorbed through the skin surface after application of the patch to the skin by means of an adhesive layer. It is estimated that currently more than one billion transdermal adhesive patches are being manufactured each year [1]. Various types of pressure-sensitive adhesive patches made from polyisobutylene, acrylic, and silicone are commercially available for use on skin [2] for applications such as smoking cessation (nicotine delivery) [3], pain relief (morphine or fentanyl delivery) [4], [5], and high blood pressure treatment (glyceryl trinitrate delivery) [6]. However, adhesive patches are associated with limitations that restrict their usage for drug delivery. These limitations include the impermeability of the outermost layer of the skin, i.e., the stratum corneum, to most hydrophilic drugs and therapeutic agents; only a few compounds of lipophilic nature can effectively be administered at useful rates using adhesive patches [7]. In addition, these patches potentially induce skin irritation upon application [8].

A transdermal approach to drug delivery using microneedles can potentially circumvent these limitations. Microneedles are solid or hollow submillimeter needle-like structures; they can be arranged in out-of-plane or in-plane arrays. Unlike traditional hypodermic needles, microneedles do not require a high level of training for drug administration, and they bear a low risk of device contamination through blood. Furthermore, they are painless since the needle tips are not required to be in direct contact with the blood vessels and the nerve endings, if they do not penetrate deep into the skin [9]–[11]. Since the early 1990s, different concepts for the fabrication of microneedles in a variety of dimensions and geometries have been developed [12]–[37]. These devices have been fabricated out of single crystal silicon [12]–[22], polysilicon [23], [24], metal [25]–[31], glass [32], and polymer (e.g., poly(methyl methacrylate) and SU-8) [33]–[37]. The lengths of the needle shafts in different arrays of out-of-plane microneedles range from 30 μm to 1 mm. Out-of-plane microneedles with solid structures have been used to increase skin permeability, while hollow microneedles are typically designed to penetrate through the stratum corneum and release an agent via their lumens into the skin.

Solid microneedles are designed to increase skin permeability by piercing the stratum corneum and exposing the underlying skin layers to the drugs that are later applied to the skin surface, or alternatively to the drugs that already coat the surface of the needles or are embedded in a biodegradable polymer that is the structural material of the needles [1], [31]. Solid microneedles provide an improvement to the existing skin patches by overcoming the stratum corneum barrier. It is shown that solid microneedles can increase skin permeability by almost four orders of magnitude [14], [31]. However, these devices provide a passive drug delivery method that might not be suitable for all applications.

Hollow microneedles can pierce through the stratum corneum and provide a passage for the injection of lipophilic and

Manuscript received June 30, 2011; revised August 26, 2011; accepted October 5, 2011. Date of publication December 12, 2011; date of current version February 3, 2012. This work was supported by the Natural Sciences and Engineering Research Council of Canada (NSERC) and the Canadian Institutes of Health Research (CIHR) through the Collaborative Health Research Projects program, as well as the British Columbia Innovation Council through the BCIC Innovation Scholarship program. This work was also supported by CMC Microsystems (www.cmc.ca) that partly funded the fabrications costs of this research through the MNT Financial Assistance program. Subject Editor L. Lin.

I. Mansoor is with the Department of Electrical and Computer Engineering, The University of British Columbia, Vancouver, BC V6T 1Z4, Canada (e-mail: imanm@ece.ubc.ca).

U. O. Häfeli is with the Faculty of Pharmaceutical Sciences, The University of British Columbia, Vancouver, BC V6T 1Z4, Canada (e-mail: urs.hafeli@ubc.ca).

B. Stoeber is with the Department of Electrical and Computer Engineering and Department of Mechanical Engineering, The University of British Columbia, Vancouver, BC V6T 1Z4, Canada (e-mail: boris.stoeber@ubc.ca).

Color versions of one or more of the figures in this paper are available online at http://ieeexplore.ieee.org.

Digital Object Identifier 10.1109/JMEMS.2011.2174429

hydrophilic compounds of small and large molecular weights into the skin. In contrast to adhesive patches, hollow microneedles are not limited by skin permeability, and unlike solid microneedles, they can be potentially used to deliver larger amounts of drugs into the skin. Transdermal drug delivery through hollow out-of-plane microneedles has been demonstrated in clinical trials, where methyl nicotinate was injected using hollow microneedles [9]. During this study, the volunteers confirmed that the method was painless and they only felt a slight pressure during the injection. In a different study, single hollow glass microneedles were used to deliver insulin to diabetic hairless rats [29]; a 30-min insulin injection at 10 or 14 psi resulted in 70% reduction in the blood glucose level over a 5-h period.

Until now, the commercial use of hollow microneedles for transdermal drug delivery has been encumbered by the expensive fabrication techniques currently used to form microneedles, such as deep reactive ion etching of silicon needles [12], [17], [19], sequential formation of disposable polymer molds for electroplating [25], [31], and multiple UV exposure or mold transfer and assembly steps to form polymer needles [33]–[37].

Here, we present a simple solvent casting method for the fabrication of hollow out-of-plane polymer microneedles [38]. Solvent casting has been a common method for more than a century to form polymer films [39]. In this method, a polymer solution is deposited onto a mold, and after evaporation of the solvent, a polymer layer remains on the mold which is then separated by mechanical force or by using chemical means. In microelectromechanical systems, solvent casting has been used to coat microchannels with polymers such as poly(vinyl alcohol), poly(ethylene oxide), polyacrylamide, and poly(N-hydroxyethylacrylamide), mainly for modifying surface properties or for protein and DNA separation [40]. Solvent casting has also been used to make polylactic acid microstructures for tissue engineering [41] as well as polystyrene microcantilever beams for sensing applications [42]. Additionally, solvent casting has been used to fabricate microneedles with solid structures [43]. We have previously shown that the polymer profile formed in a mold during solvent casting can be adjusted by controlling the solvent casting process parameters such as temperature [44].

Solvent casting is a fast and repeatable fabrication process for microneedles, and it requires only one step of photolithography, eliminating the need for mask alignment. Here, we present the selection of the clay concentration for maximum strength of the polymer-clay composite that serves as the structural material for the needles, followed by the detailed fabrication process of the microneedles made using solvent casting. This is then followed by a study of the mechanical strength of the fabricated microneedles, and by the demonstration of fluid injection into rabbit ear skin.

II. Fabrication of Hollow Out-of-Plane Polymer Microneedles

A. Microneedle Material Selection

Polyimide was chosen as the structural material for the microneedles due to its high Young's modulus (8.5 GPa) relative to the highest Young's modulus of biocompatible polymer materials [45]. The polyimide type PI-2611 (HD Microsystems, Parlin, NJ) used in this work was diluted with its solvent N-methyl-2-pyrrolidone (NMP) for better deposition and handling, at a weight ratio of 4 : 3 (PI-2611 : NMP). To further increase the strength and rigidity of the polyimide, montmorillonite nanoclay powder (Nanocor, Hoffman Estates, IL) was added to the polymer as reinforcement. A series of tests was performed to determine the optimum clay percentage in the polyimide that would result in the highest strength under compressive loading. For preparing the composite mixtures, first, the nanoclay powder was mixed with the polyimide solvent NMP for 5 s using a Model 100 Sonic Dismembrator (Fisher Scientific) at 5 W output power. Then, this suspension was added to the PI-2611 polyimide solution and mixed using a stir bar for several minutes. The mechanical tests were performed on cone-shaped test structures made through solvent casting the polyimide-nanoclay composite from a polydimethylsiloxane (PDMS) mold. For each investigated clay percentage in the composite, three test structures were created using the same mold. The structures were 280 μm tall and had tip and base diameters of 65 μm and 115 μm, respectively. To apply compressive loads, a Physica MCR rheometer (Anton Paar, Ashland, VA) was used, which recorded force versus displacement for each compression test (Fig. 1). The rheometer's test geometry

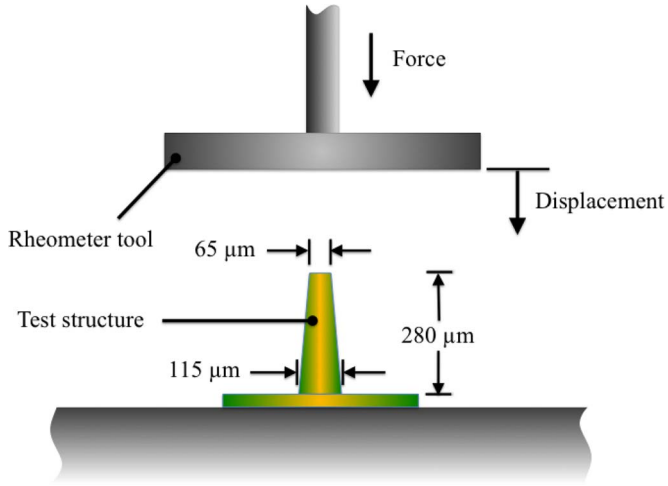

Fig. 1. Setup used for compression tests.

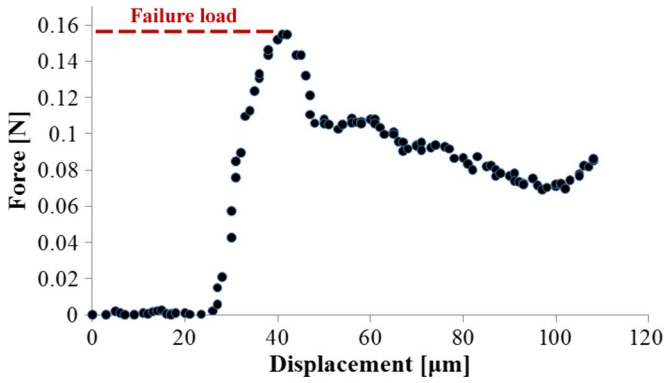

Fig. 2. Typical compression test curve for a test structure with 2 wt% clay reinforcement.

TABLE I
MEAN FAILURE LOADS FOR DIFFERENT CLAY CONTENT IN POLYIMIDE, OBTAINED FROM THREE TESTS PER CLAY CONTENT

Clay content [weight %]	0	1	2	3	4	5	10
Average failure load [N]	0.144	0.109	0.169	0.130	0.127	0.107	0.153
Standard deviation [N]	0.009	0.014	0.016	0.006	0.012	0.011	0.010

was set to move vertically downwards onto the test structures at a constant velocity of 2 μm/s. The force was recorded at a resolution of 1 mN.

An example of a force versus displacement graph is shown in Fig. 2. In this plot, the sharp peak corresponds to the failure load that leads to bending of the structure under compressive stress. The test results showed that the drop in force after the peak is steeper for higher clay content, indicating a more brittle behavior. The average of the maximum failure loads for the different clay contents are shown in Table I, which indicates that the 2 wt% clay reinforced polyimide has the highest failure load and was therefore chosen as the composite for the fabrication of microneedles.

B. Fabrication Process

The epoxy-type negative photoresist SU-8 (Microchem, Newton, MA) was used for the mold. For fabrication of the mold, a 450 μm layer of SU-8 2150 was first spin coated on a 300 μm thick Pyrex glass substrate, and then soft-baked on a hotplate at 65 °C for 10 min and at 95 °C for 2 h. The SU-8 was then exposed to 5300 mJ cm^{-2} UV light (performed in several 2-min intervals with 20-s cooling breaks in between) through a dark field mask that contained arrays of circular transparent regions with diameter of 40 μm. The exposure was performed through the Pyrex substrate, as shown in Fig. 3(a), to take advantage of light diffraction caused by the gap between the mask and the photoresist [46]. This method of exposure resulted in tapered pillar structures with the wider bases attached to the Pyrex base plate. After exposure, the sample was baked on a hotplate at 65 °C for 5 min and at 95 °C for 25 min. Next, the sample was immersed in SU-8 developer for approximately 45 min and then rinsed for 5 min with fresh developer and isopropanol. The resulting structure was an array of slightly tapered cylindrical pillars (Figs. 3(b) and 4) with base diameters of 60 μm, tip diameters of 40 μm, and a center-to-center spacing of 500 μm. These pillars constituted the mold, and they would eventually form the lumens of the needles. The entire mold structure was then coated with a 4 μm layer of Parylene C (Specialty Coating Systems, Indianapolis, IN). This layer improved adhesion of the pillars to the Pyrex substrate and provided a protective surface on the mold for consecutive fabrication steps. Consecutively, a thin layer of PDMS (Dow Corning, Midland, MI) was spin coated onto the mold structure at a base layer thickness of 30 μm and cured at 65 °C for 2 h. This layer improved the strength and rigidity of the mold structure and also had a poor adhesion with the structural material of the microneedles, which therefore allowed easy removal of the microneedle array from the mold [Fig. 3(c)]. The complete mold structure contained an array of 14 pillars and was surrounded by a square (8 mm × 8 mm) of vertical walls (Fig. 5). The mold structure at this stage could be used for consecutive solvent casting of microneedles.

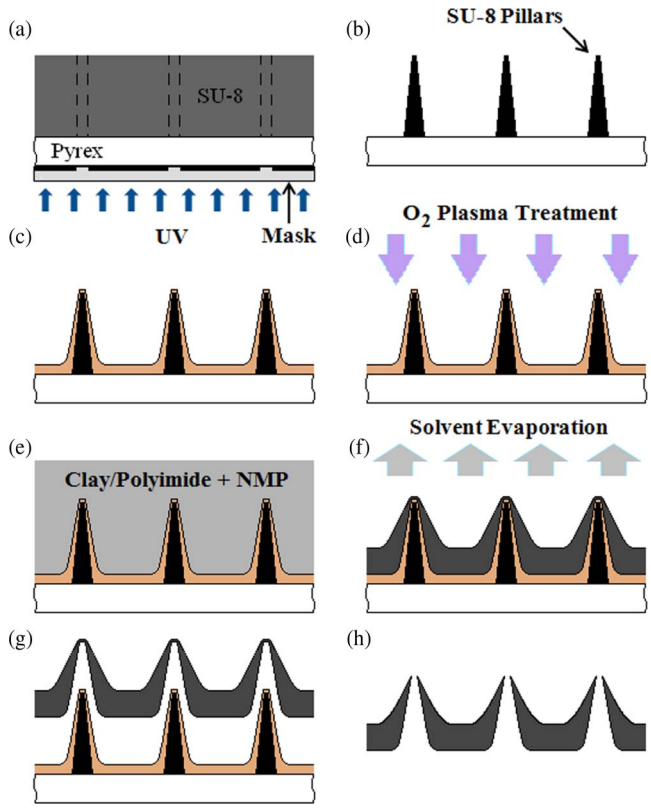

Fig. 3. Fabrication process using solvent casting for hollow out-of-plane polymer microneedles, (a) and (b) fabrication of pillars from SU-8, (c) PDMS deposition, (d) O_2 plasma treatment of the mold, (e) deposition of a clay/polyimide suspension in NMP, (f) Evaporation of NMP, (g) removing of the microneedle array from the mold, and (h) opening of the microneedle tips.

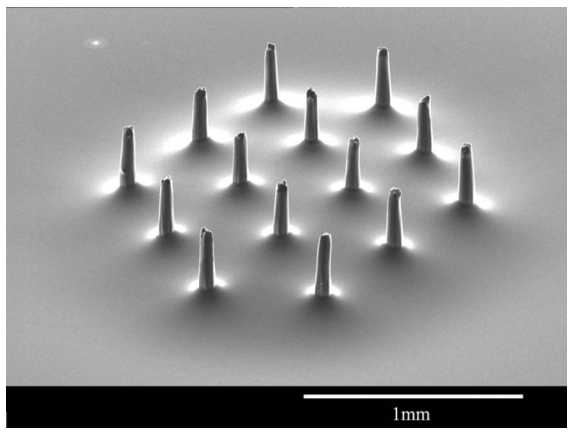

Fig. 4. SEM image of an array of pillars in a mold used for microneedle fabrication.

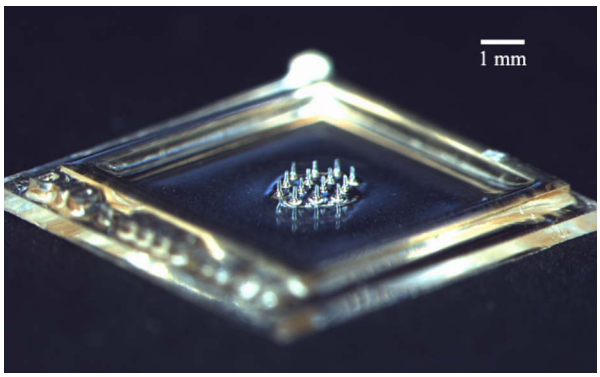

Fig. 5. Complete mold used for microneedle fabrication.

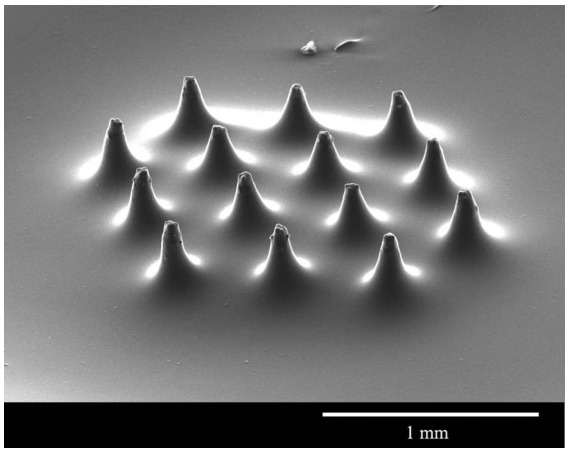

Fig. 6. SEM image of an array of solid microneedles formed in a mold after solvent evaporation.

For fabrication of the microneedle arrays, first, the mold was treated for 30 s with O_2 plasma in a RIE/PECVD tool (Trion Technology, Clearwater, FL), with a power setting of 30 W, an oxygen flow rate of 50 sccm, and a chamber pressure of 500 mTorr. The plasma treatment temporarily improved the surface wetting of PDMS by the polymer solution used for solvent casting and therefore resulted in sharper and taller needles. Without plasma treatment, the polymer solution does not cover the pillars entirely and leads to shorter and blunter structures. Consecutively, 35 μL of the 2% clay polyimide/NMP mixture was deposited into the mold structure [Fig. 3(e)]. During a soft baking process in an oven at 65°C for 2 h, NMP evaporated, and the microneedles were formed around the pillars in the mold with wide bases and sharp tips (Figs. 3(f) and 6). The obtained structures would be suitable for use as solid out-of-plane microneedles, in which case the molds would not be reusable for consecutive fabrication.

To achieve hollow structures, the array was separated from the mold by mechanical force [Fig. 3(g)]. It was observed that the separation of the polyimide/clay layer became easier if sufficient time had passed after the soft baking process (more than 48 h), which may have been due to a slight swelling of the polymer film due to moisture uptake [47]–[49] or deformation due to further solvent evaporation at room temperature. After separating the needle structure from the mold, a thin layer of the polyimide/clay composite resided on top of the needles from the polymer solvent casting step obstructing the needle lumen. This layer was removed [Fig. 3(h)] by either an O_2/CF_4 plasma etching step (200 W power, 700 mTorr pressure, 80 sccm O_2, 20 sccm CF_4, and duration of 300–500 s at 25 °C) or by polishing the tips using fine 3 μm aluminum oxide polishing film (3M, St. Paul, MN).

Fig. 7 shows SEM images of the microneedles fabricated through this process. Fig. 7(a) shows an array of 250 μm long microneedles with tip diameters of 50.4 ± 4.2 μm (mean $\pm$ standard deviation) and the same pitch of 500 μm as the pillars. The slight variation in the microneedle tip diameter is mainly due to the variation in thickness of the spin-coated PDMS layer on the SU-8 pillars, which may lead to small differences in the force required for the penetration of the microneedles into skin. Wider bases of pillars, due to the backside exposure of the SU-8, result in larger channel openings on the backside of the backing plate as shown in Fig. 7(b). In Fig. 7(c), a single microneedle is shown with its tip opened through plasma etching, while Fig. 7(d) shows a single microneedle with the tip opened by sanding.

The dimensions of the microneedles can be adjusted by changing the dimensions of the mold structure during the photolithography steps. For instance, longer pillars with smaller diameter result in longer needles with smaller channel diameters.

C. Contact Angle Measurement of NMP on a PDMS Surface

To characterize the polyimide-PDMS interaction after plasma treatment of the mold and during solvent casting, a series of tests was performed to observe the change in contact angle of polyimide solvent on a PDMS surface over time after the PDMS is plasma treated and covered with a layer of polyimide, as during the casting step in the fabrication process as shown in Fig. 3(e) and (f). For these tests, first a layer of PDMS was spin coated on a microscope slide and then baked to cure. The PDMS surface was then treated with oxygen plasma as explained above. A thin layer of polyimide was then spin coated on the PDMS surface and left in an oven to soft bake at 65°C for 2 h. The polyimide layer was peeled off from different samples after different time intervals (6 h, 8 h, 1 day, 2 days, 3 days, and 6 days) following solvent casting. The advancing contact angle was measured immediately after peeling off the polyimide layer from the PDMS surface [Fig. 8(a)] using a Theta tensiometer (Attension/Biolin Scientific, Espoo, Finland). The measurements were performed on 4 μL NMP droplets and were repeated several times over the duration of 30 min, each time in a different location on the PDMS sample.

Fig. 8(b) shows the measurement results. It was observed that regardless of when the polyimide layer was removed, the immediate contact angle of NMP on PDMS was constant and low (about 10–15°). The angle only increased when the surface was in contact with air, and this increase occurred at a similar rate regardless of how long after solvent casting the polyimide layer was removed.

This showed that the surface wetting behavior of NMP on PDMS remains identical throughout the evaporation process,

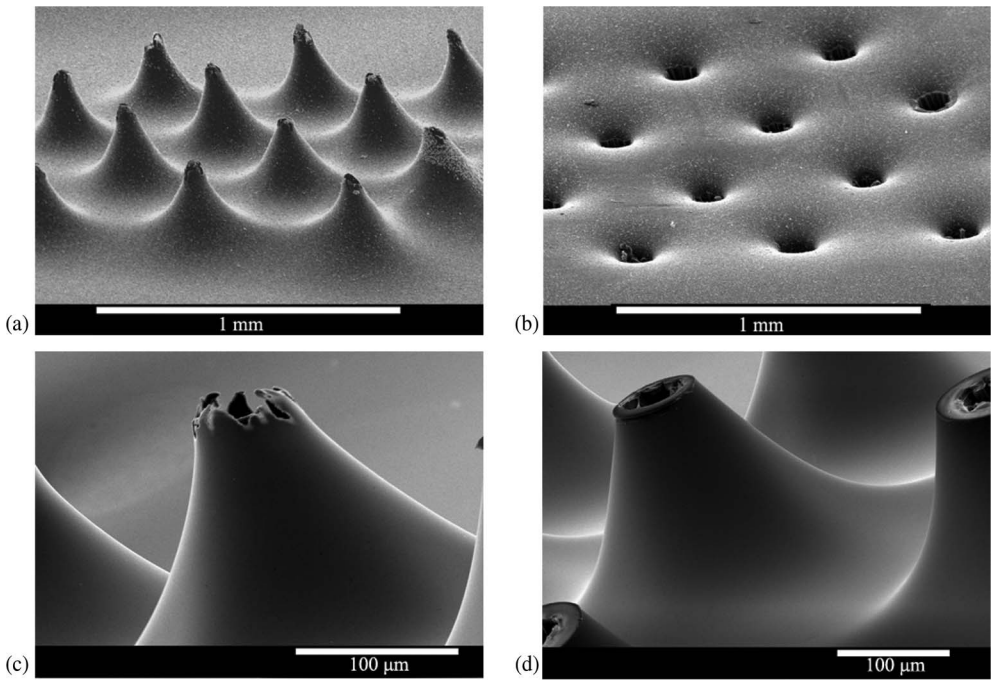

Fig. 7. SEM images of fabricated microneedles: (a) Array of 250 μm long needles, (b) microneedle channel openings, (c) a needle tip opened by plasma etching, and (d) a needle tip opened by sanding.

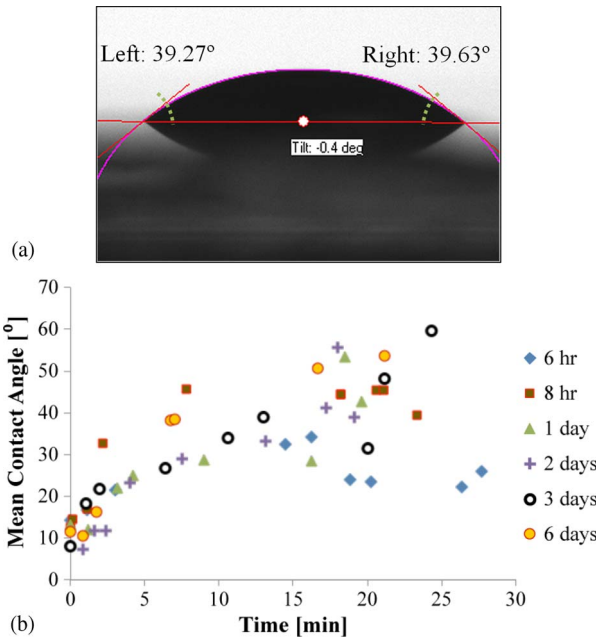

Fig. 8. NMP contact angle on a PDMS surface. (a) Contact angle measured 3 days after the PDMS surface was coated with a polyimide layer, 13 min after removing the polyimide layer. (b) Contact angle measurements for NMP on PDMS at different times after removing a polyimide layer that was deposited between 6 h and 6 days prior to removal.

which would result in needles with the desired geometry; the wetting behavior of NMP on PDMS also remains constant as long as the PDMS surface is in contact with the polyimide composite layer. The wetting only changes when the PDMS is in contact with air, regardless of when the polyimide composite is removed from the PDMS surface.

III. Experimental Procedures for Needle Characterization

A. Microneedle Robustness Tests

To test the robustness of the fabricated microneedles, a series of compression tests were performed on individual 2 wt% clay-reinforced polyimide needles, with tips opened by plasma etching. The test procedures were identical to the robustness tests performed on test structures described in Section II-A. Individual needles were made using the process shown in Fig. 3. A total of ten 250 μm-long needles were tested under compressive loading, and the corresponding force versus displacement plots were obtained for each test.

B. Microneedle Injection Tests

The capability of the fabricated devices for drug delivery and skin penetration was demonstrated through injection trials on rabbit ear skin. Rabbit ear skin was used for this study because it is a reasonable human skin model for in vitro transdermal permeation studies [50]. Traditionally, pig skin has been used as a skin model for permeation studies due to its biochemical similarity with human skin [51], [52]. However, pig skin and other traditional skin models are associated with a high permeability compared to human skin, particularly when it comes to hydrophilic agents. In contrast, rabbit ear skin has a considerably lower permeability to hydrophilic compounds compared with traditional skin models, and is therefore considered to be a more suitable human skin model for *in vitro* trials [50].

Arrays of 250 μm-long microneedles, with tips opened by plasma etching, were bonded to modified plastic female luer-to-barb fittings (McMaster-Carr, Cleveland, OH), using Loctite

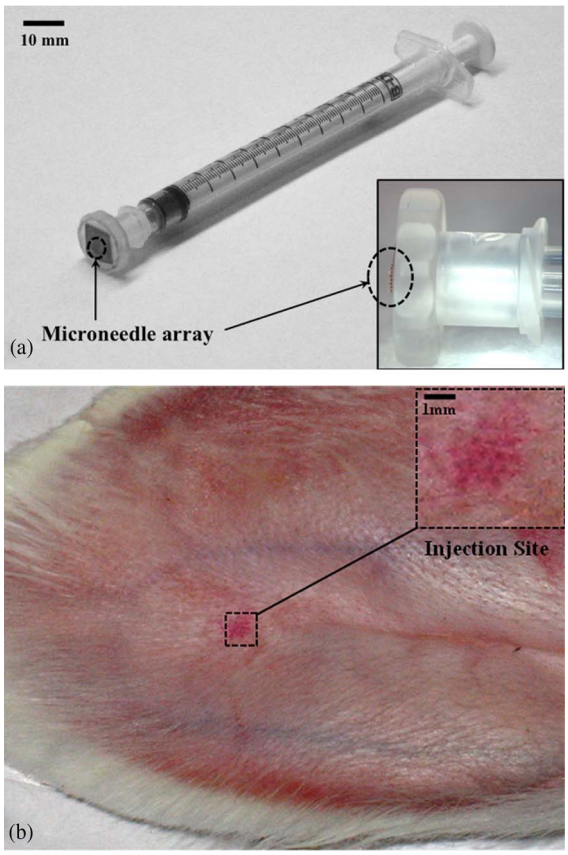

Fig. 9. (a) A microneedle array attached to a syringe. (b) Rabbit ear skin after application of the microneedles.

Super Glue (Henkel, Avon, OH), and then attached to conventional 1-mL syringes (Becton Dickinson, Mississauga, ON) as shown in Fig. 9(a). A 0.025 wt% suspension of 0.21 μm polystyrene fluorescent beads (Bangs Laboratories, Fishers, IN) in water was prepared. For each trial, the syringes were filled with the suspension containing fluorescent beads and then were pressed against the inner rabbit ear skin for about 10 s, while a moderate pressure was applied to the plunger. Fig. 9(b) shows the skin after application of the microneedles. A total of six injection trials were carried out. After each test, the injection site was imaged using a D-Eclipse C1 confocal microscope (Nikon). Using the confocal microscope, the skin was scanned down to a depth of 200 μm to investigate the penetration of the fluorescent beads under the skin.

IV. Results and Discussion

A. Microneedle Robustness

Fig. 10(a) shows an example of a force versus displacement plot obtain for a compression test on a needle. The plot shows a sudden increase in force upon contact with the microneedles tip followed by a sudden drop in force. The peak force corresponds to the failure load of the microneedle similar to the force variation seen for the solid structures in Fig. 2. A needle tip after failure is shown in Fig. 10(b). In this figure, the tip of the microneedle has collapsed and bent almost at the midpoint of the needle shaft, while the needle base is still rigid, which

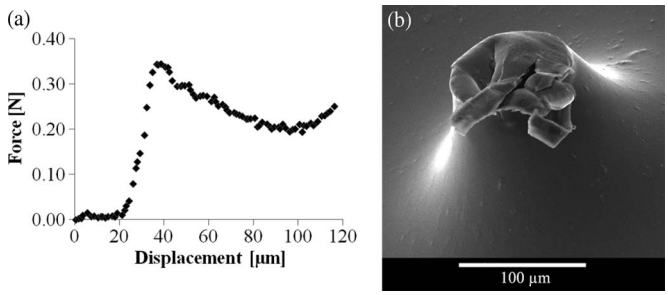

Fig. 10. (a) A needle displacement under axial loading. (b) A failed needle after loading.

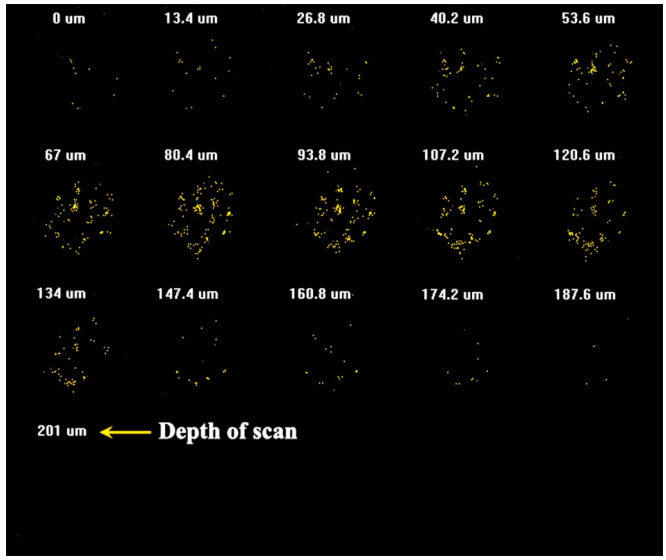

Fig. 11. Confocal scan of skin after injection of fluorescent beads. The skin surface is at 0 μm. The confocal slice thickness is 13.4 μm.

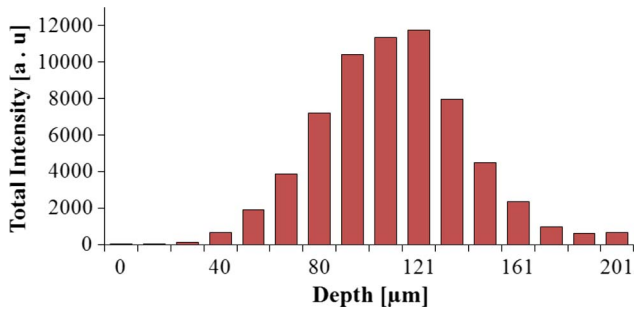

Fig. 12. Histogram of the intensity distribution of the fluorescent beads obtained from the confocal scan in Fig. 11.

explains the increase in force again as the needle is compressed further. From these tests, it was observed that on average, the microneedles can sustain compressive loads of up to 0.32 $\pm$ 0.06 N (mean $\pm$ standard deviation).

Davis *et al.* investigated the relationship between the cross-sectional area of a microneedle tip (interfacial area) and the force required for penetration of the microneedle into skin [53]. The experimental results presented by Davis *et al.* seem to suggest that the needle strength obtained experimentally for polymer/clay composite needles with a 50 μm tip diameter in this work, $F_N = 0.32$ N, is sufficient to penetrate human skin.

TABLE II
MEAN INJECTION DEPTH AND 95% CONFIDENCE INTERVAL FOR THE FLUORESCENCE INTENSITY DISTRIBUTION OF INJECTED BEADS AS IN FIG. 12

Trial	1	2	3	4	5	6	Average
Mean depth [μm]	110.3	113.9	83.7	108.7	123.9	88.1	104.8
Upper range [μm]	169.4	176.7	121.8	171.0	180.3	166.3	164.3
Lower range [μm]	51.3	51.1	45.5	46.4	67.4	9.9	45.3

B. Results of Injection Tests

Fig. 11 shows the fluorescent beads at different depths under the skin surface after an injection test using microneedles. For each confocal scan, an intensity histogram distribution was obtained by measuring the total bead fluorescent intensity at each depth using MATLAB for image processing. Fig. 12 shows the intensity distribution for the confocal scan shown in Fig. 11.

For each injection test, an average penetration depth and a penetration range were calculated from these intensity measurements corresponding to the mean and the 95% confidence interval, respectively. The results from six injection trials are shown in Table II. The average delivery depth for all the trials was 104.8 ± 15.6 μm with an average range of 119 ± 25.8 μm, indicating successful delivery into the epidermis, past the stratum corneum.

Since the microneedles used for these tests are 250 μm long, the average delivery depth of 104.8 μm indicates that the majority of the microneedle height could not penetrate due to the flexibility of the skin. This penetration behavior might be different for human skin, and additional experiments have to be done *in vivo* to observe the penetration depth in human skin. Additionally, in all of the confocal images, the distribution of the fluorescent beads was localized to distinct regions corresponding to each individual needle in the array. The distance between the needles therefore seems to be sufficient to have them act independently as individual needles, and injection of more material, with controlled volume, could thus be accomplished by proportionally adding more needles.

V. CONCLUSION

A new fabrication technique, based on solvent casting, has been presented for fabrication of hollow out-of-plane microneedles on a reusable mold. This fabrication procedure is inexpensive and applicable for mass production of polymer microneedles. The proposed process is flexible in terms of the possible dimensions of the microneedle array as well as the needle material. By adjusting the photolithography parameters and therefore controlling the pillar dimensions in the mold, microneedles with various heights and lumen diameters can be made. Also, other polymers can be used in this process for hollow microneedle fabrication by adjusting the process parameters.

Clay-reinforced polyimide was used in the proposed process to fabricate 250 μm long microneedles. A series of compression tests were carried out on solid structures to find the optimum clay percentage in the composite, leading to the maximum compressive strength. The robustness of the fabricated microneedles has been measured, and the needles were found to be strong enough for penetration into rabbit skin. The delivery of a suspension of polystyrene beads into the epidermis was successfully demonstrated.

REFERENCES

[1] M. R. Prausnitz and R. Langer, "Transdermal drug delivery," *Nat. Biotechnol.*, vol. 26, no. 11, pp. 1261–1268, Nov. 2008.
[2] S. Venkatraman and R. Gale, "Skin adhesives and skin adhesion: 1. Transdermal drug delivery systems," *Biomaterials*, vol. 19, no. 13, pp. 1119–1136, Jun. 1998.
[3] S. K. Govil and P. Kohiman, "Transdermal delivery of nicotine," U.S. Patent 4 908 213, Mar. 13, 1990.
[4] K. J. Miller, S. K. Govil, and K. S. Bhatia, "Fentanyl suspension-based silicone adhesive formulations and devices for transdermal delivery of fentanyl," U.S. Patent 7 556 823, Feb. 12, 2009.
[5] T. T. Takeshi and H. Naruhito, "Transdermal patch for external use compromising fentanyl," Int. Patent WO/2004/035054, 2004.
[6] S. K. Govil, E. M. Rudnic, and D. G. Sterner, "Transdermal nitroglycerin patch with penetration enhancers," U.S. Patent 5 262 165, Nov. 16, 1993.
[7] N. Y. N. Kalia and R. H. Guy, "Transdermal drug delivery: Overcoming the skin's barrier function," *Pharm. Sci. Technol. Today*, vol. 3, no. 9, pp. 318–326, Sep. 2000.
[8] M. Murphy and A. J. Carmichael, "Transdermal drug delivery systems and skin sensitivity reactions: Incidence and management," *Amer. J. Clin. Dermatol.*, vol. 1, no. 6, pp. 361–368, Nov./Dec. 2000.
[9] R. K. Sivamani, B. Stoeber, G. C. Wu, H. Zhai, D. Liepmann, and H. Maibach, "Clinical microneedle injection of methyl nicotinate: Stratum corneum penetration," *Skin Res. Technol.*, vol. 11, no. 2, pp. 152–156, May 2005.
[10] S. Kaushik, A. H. Hord, D. D. Denson, D. V. McAllister, S. Smitra, M. G. Allen, and M. R. Prausnitz, "Lack of pain associated with microfabricated microneedles," *Anesth. Analgesia*, vol. 92, no. 2, pp. 502–504, Feb. 2001.
[11] H. S. Gill, D. D. Denson, B. A. Burris, and M. R. Prausnitz, "Effect of microneedle design on pain in human volunteers," *Clin. J. Pain*, vol. 24, no. 7, pp. 585–594, Sep. 2008.
[12] B. Stoeber and D. Liepmann, "Arrays of hollow out-of-plane microneedles for drug delivery," *J. Micorelectromech. Syst.*, vol. 14, no. 3, pp. 472–479, Jun. 2005.
[13] S. J. Paik, S. Byun, J. M. Lim, Y. Park, A. Lee, S. Chung, J. Chang, K. Chun, and D. Cho, "In-plane single-crystal-silicon microneedles for minimally invasive microfluid systems," *Sens. Actuators A, Phys.*, vol. 114, pp. 276–284, 2004.
[14] S. Henry, D. V. Mcallister, M. G. Allen, and M. R. Prausnitz, "Microfabricated microneedles: A novel approach to transdermal drug delivery," *J. Pharm. Sci.*, vol. 87, no. 8, pp. 922–925, Aug. 1998.
[15] W. Martanto, S. Davis, N. Holiday, J. Wang, H. Gill, and M. Prausnitz, "Transdermal delivery of insulin using microneedles in vivo," *Pharm. Res.*, vol. 21, no. 6, pp. 947–952, Jun. 2004.
[16] J. A. Mikszta, J. B. Alarcon, J. M. Brittingham, D. E. Sutter, R. J. Pettis, and N. G. Harvey, "Improved genetic immunization via micromechanical disruption of skinbarrier function and targeted epidermal delivery," *Nat. Med.*, vol. 8, no. 4, pp. 415–419, Apr. 2002.
[17] H. J. G. E. Gardeniers, R. Luttge, E. J. W. Berenschot, M. J. de Boer, S. Y. Yeshurun, M. Hefetz, R. van't Oevera, and A. van den Berg, "Silicon micromachined hollow microneedles for transdermal liquid transport," *J. Micorelectromech. Syst.*, vol. 12, no. 6, pp. 855–862, 2003.

[18] J. Brazzle, D. Bartholomeusz, R. Davies, and J. Andrade, "Active microneedles with integrated functionality," in *Proc. Solid State Sens. Actuators Workshop*, Hilton Head, SC, 2000, pp. 199–202.
[19] J. Ji, F. E. H. Tay, and J. Miao, "Microfabricated hollow microneedle array using ICP etcher," *J. Phys., Conf. Ser.*, vol. 34, no. 34, pp. 1132–1136, May 2006.
[20] P. Griss and G. Stemme, "Side-opened out-of-plane microneedles for microfluidic transdermal liquid transfer," *J. Micorelectromech. Syst.*, vol. 12, no. 3, pp. 296–301, Jun. 2003.
[21] E. V. Mukerjee, S. D. Collins, R. R. Isseroff, and R. L. Smith, "Microneedle array for transdermal biological fluid extraction and in situ analysis," *Sens. Actuators A, Phys.*, vol. 114, no. 2/3, pp. 267–275, Sep. 2004.
[22] M. Shikida, M. Ando, Y. Ishihara, T. Ando, K. Sato, and K. Asaumi, "Nonphotolithographic pattern transfer for fabricating pen-shaped microneedle structures," *J. Micromech. Microeng.*, vol. 14, no. 11, pp. 1462–1467, Nov. 2004.
[23] J. D. Zahn, N. H. Talbot, D. Liepmann, and A. P. Pisano, "Microfabricated polysilicon microneedles for minimally invasive biomedical devices," *Biomed. Microdevices*, vol. 2, no. 4, pp. 295–303, Dec. 2000.
[24] K. Chun, G. Hashiguchi, H. Toshiyoshi, and H. Fujita, "Fabrication of array of hollow microcapillaries used for injection of genetic materials into animal/plant cells," *Jpn. J. Appl. Phys.*, vol. 38, no. 3A, pp. L279–L281, Mar. 1999.
[25] K. Kim, D. S. Park, H. M. Lu, W. Che, K. Kim, J. Lee, and C. H. Ahn, "A tapered hollow metallic microneedle array using backside exposure of SU-8," *J. Micromech. Microeng.*, vol. 14, no. 4, pp. 597–603, Apr. 2004.
[26] J. A. Matriano, M. Cormier, J. Johnson, W. A. Young, M. Buttery, K. Nyam, and P. E. Daddona, "Macroflux microprojection array patch technology: A new and efficient approach for intracutaneous immunization," *Pharm. Res.*, vol. 19, no. 1, pp. 63–70, Jan. 2002.
[27] S. Chandrasekaran and A. B. Frazier, "Characterization of surface micromachined metallic microneedles," *J. Microelectromech. Syst.*, vol. 12, no. 3, pp. 289–295, Jun. 2003.
[28] J. D. Brazzle, I. Papautsky, and A. B. Frazier, "Hollow metallic micromachined needle arrays," *Biomed. Microdevices*, vol. 2, no. 3, pp. 197–205, Jun. 2000.
[29] S. P. Davis, W. Martanto, M. Allen, and M. Prausnitz, "Hollow metal microneedles for insulin delivery to diabetic rats," *IEEE Trans. Biomed. Eng.*, vol. 52, no. 5, pp. 909–915, May 2005.
[30] K. Kobayashi and H. Suzuki, "A sampling mechanism employing the phase transition of a gel and its application to a micro analysis system imitating a mosquito," *Sens. Actuators B, Chem.*, vol. 80, no. 1, pp. 1–8, Nov. 2001.
[31] D. V. McAllister, P. M. Wang, S. P. Davis, J.-H. Park, P. J. Canatella, M. G. Allen, and M. R. Prausnitz, "Microfabricated needles for transdermal delivery of macromolecules and nanoparticles: Fabrication methods and transport studies," *Proc. Nat. Acad. Sci. USA*, vol. 100, no. 24, pp. 13 755–13 760, Nov. 2003.
[32] K. T. Brown and D. G. Flaming, *Advanced Micropipette Techniques for Cell Physiology*. New York: Wiley, 1986.
[33] S. J. Moon, S. S. Lee, H. S. Lee, and T. H. Kwon, "Fabrication of microneedle array using LIGA and hot embossing process," *Microsyst. Technol.*, vol. 11, no. 4/5, pp. 311–318, Apr. 2005.
[34] J. Park, M. G. Allen, and M. R. Prausnitz, "Biodegradable polymer microneedles: Fabrication, mechanics and transdermal drug delivery," *J. Controlled Release*, vol. 104, no. 1, pp. 51–66, May 2005.
[35] M. Han, D. Hyun, H. Park, S. S. Lee, C. Kim, and C. Kim, "A novel fabrication process for out-of-plane microneedle sheets of biocompatible polymer," *J. Micromech. Microeng.*, vol. 17, no. 6, pp. 1184–1191, Jun. 2007.
[36] H. Huang and C. Fu, "Different fabrication methods of out-of-plane polymer hollow needle arrays and their variations," *J. Micromech. Microeng.*, vol. 17, no. 2, pp. 393–402, Feb. 2007.
[37] S. Kuo and Y. Chou, "A novel polymer microneedle arrays and PDMS micromolding technique," *Tamkang J. Sci. Eng.*, vol. 7, no. 2, pp. 95–98, 2004.
[38] I. Mansoor, U. O. Häfeli, and B. Stoeber, "Arrays of solvent cast hollow out-of-plane polymer microneedles for drug delivery," in *Proc. IEEE 24 Int. Conf. MEMS*, 2011, pp. 1027–1030.
[39] U. Siemann, "Solvent cast technology—A versatile tool for thin film production," *Prog. Colloid Polym. Sci.*, vol. 130, pp. 1–14, 2005.
[40] E. A. S. Doherty, R. J. Meagher, M. N. Albarghouthi, and A. E. Barron, "Microchannel wall coatings for protein separations by capillary and chip electrophoresis," *Electrophoresis*, vol. 24, no. 1/2, pp. 34–54, Jan. 2003.
[41] G. J. Wang, K. H. Ho, and C. C. Hsueh, "Biodegradable polylactic acid microstructures for scaffold applications," *Microsyst. Technol.*, vol. 14, no. 7, pp. 989–993, Jul. 2008.
[42] A. W. McFarland, M. A. Poggi, L. A. Bottomley, and J. S. Colton, "Production and characterization of polymer microcantilevers," *Rev. Sci. Instrum.*, vol. 75, no. 8, pp. 2756–2758, Aug. 2004.
[43] J. W. Lee, J.-H. Park, and M. R. Prausnitz, "Dissolving microneedles for transdermal drug delivery," *Biomaterials*, vol. 29, no. 13, pp. 2113–2124, May 2008.
[44] I. Mansoor and B. Stoeber, "PIV measurements of flow in drying polymer solutions during solvent casting," *Exp. Fluids*, vol. 50, no. 5, pp. 1409–1420, May 2011.
[45] HD Microsystems, *PI-2600 Series—Low Stress Applications*, 2009, Product Bulletin. [Online]. Available: http://hdmicrosystems.com/HDMicroSystems/en_US/pdf/PI-2600_ProcessGuide.pdf
[46] M. C. Peterman, P. Huie, D. M. Bloom, and H. A. Fishman, "Building thick photoresist structures from the bottom up," *J. Micromech. Microeng.*, vol. 13, no. 3, pp. 380–382, May 2003.
[47] C. Jang, S. Yoon, and B. Han, "Measurement of the hygroscopic swelling coefficient of thin film polymers used in semiconductor packaging," *IEEE Trans. Compon. Packag. Technol.*, vol. 33, no. 2, pp. 340–346, Jun. 2010.
[48] S. C. Noe, J. Y. Pan, and S. D. Senturia, "Optical waveguiding as a method for characterizing the effect of extended cure and moisture on polyimide films," *Polym. Eng. Sci.*, vol. 32, no. 15, pp. 1015–1020, Aug. 1992.
[49] H. L. Tyan, C. Y. Wu, and K. H. Wei, "Effect of montmorillonite on thermal and moisture absorption properties of polyimide of different chemical structures," *J. Appl. Polym. Sci.*, vol. 81, no. 7, pp. 1742–1747, Aug. 2001.
[50] S. Nicoli, C. Padula, V. Aversa, B. Vietti, P. W. Wertz, A. Millet, F. Falson, and R. P. Feynman, "Characterization of rabbit ear skin as a skin model for in vitro transdermal permeation experiments: Histology, lipid composition and permeability," *Skin Pharmacol. Physiol.*, vol. 21, no. 4, pp. 218–226, Jul. 2008.
[51] P. Dick and R. C. Scott, "Pig ear skin as an in-vitro model for human skin permeability," *J. Pharm. Pharmacol.*, vol. 44, no. 8, pp. 640–645, Aug. 1992.
[52] N. Sekkat, Y. N. Kalia, and R. H. Guy, "Biophysical study of porcine ear skin in vitro and its comparison to human skin in vivo," *J. Pharm. Sci.*, vol. 91, no. 11, pp. 2376–2381, Nov. 2002.
[53] S. P. Davis, B. J. Landis, Z. H. Adams, M. G. Allen, and M. R. Prausnitz, "Insertion of microneedles into skin: Measurement and prediction of insertion force and needle fracture force," *J. Biomech.*, vol. 37, no. 8, pp. 1155–1163, Aug. 2004.

Iman Mansoor was born in Shiraz, Iran, in 1984. He received the Bachelor's degree in mechanical engineering, mechatronics option, and the Master's degree in electrical engineering, both from The University of British Columbia, Vancouver, BC, Canada, in 2007 and 2009, respectively. Since January 2010, he has been working toward the Ph.D. degree in electrical engineering at The University of British Columbia.

His research interests include bioMEMS, MEMS drug delivery systems, biomaterials, MEMS fabrication technologies, polymer composites, and solvent casting of polymer films.

Urs O. Häfeli received the B.Sc. degree in pharmacy from the Swiss Federal Institute of Technology, Zurich, Switzerland, in 1986, and the Ph.D. degree from the Paul Scherrer Institute, Villigen, Switzerland, in 1989.

He spent 1.5 years as a Postdoctoral Fellow at the Joint Center of Radiation Therapy at Harvard University, followed by 11 years as a Research Scientist in the Radiation Oncology Department of the Cleveland Clinic Foundation. He is currently an Associate Professor in the Faculty of Pharmaceutical Sciences at The University of British Columbia, Vancouver, BC, Canada. His research has concentrated on magnetic drug targeting with microspheres and nanospheres and on the preparation of biocompatible and biodegradable monosized particles. To make uniform particles, he is investigating flow focusing based on silica and polydimethylsiloxane nanotechnologies. The overall aim is to use drug releasing targeted particles for radiopharmaceutical cancer therapy. Every two years, since 1996, he has organized and co-chaired the International Conference on the Scientific and Clinical Applications of Magnetic Carriers. At its last meeting in May 2010, the conference attracted 370 participants from 43 countries to Rostock, Germany.

Boris Stoeber (M'06) received the electrical engineering Diploma from the Technische Universität Darmstadt, Darmstadt, Germany, in 1998, the general engineering Diploma from the École Centrale de Lyon, Ecully, France, in 1998, and the Ph.D. degree in mechanical engineering from the University of California, Berkeley, in 2002.

From 2003 to 2005, he was a Postdoctoral Scientist in chemical engineering at the University of California, Berkeley. Since 2005, he has been with the Department of Mechanical Engineering and the Department of Electrical and Computer Engineering at The University of British Columbia, Vancouver, BC, Canada. His research interests include microflow control strategies, flow physics of complex microflows, microflow imaging methods, microoptical devices, sensing technology, biomedical microdevices, and fabrication techniques for microelectromechanical structures.

Dr. Stoeber is a member of the Society of Rheology. He is an Associate Editor for the IEEE SENSORS JOURNAL.